Reprinted from "Boundary Layer and Flow Control"

PERGAMON PRESS

OXFORD · LONDON · NEW YORK · PARIS

1961

PROGRESS IN THE DESIGN OF LOW DRAG AEROFOILS

By F. X. WORTMANN

1. INTRODUCTION

THE properties of an aerofoil section can best be assessed from its velocity distribution. From the known velocity distribution at a given angle of incidence follow approximately the lift and moment of the aerofoil section; the velocity distributions for other angles of incidence can be derived by potential theory. With some experience it is possible to indicate broadly the shape and thickness of the wing section without detailed calculation. Finally—and this is the main reason why the starting point for the design of a modern aerofoil section is always the velocity distribution—it is only possible to discuss theoretically the development of the boundary layer in these terms and thereby obtain drag and the polar diagram (lift–drag curve) of the aerofoil section. The design of an aerofoil section, therefore, consists of selecting from the large number of possible velocity distributions those which will lead to an aerofoil section approximating most closely to the requirements in respect of shape and aerodynamic characteristics. The process of selection presupposes the existence of theoretical methods suitable for evaluating the shape of the wing section and the character of the boundary layer from the velocity distribution, it demands, in parallel, a careful experimental check of theoretical method and deductions. The well-known N.A.C.A. laminar or low-drag aerofoils, which were developed some fifteen years ago in the U.S.A., were the first aerofoils for which the velocity distribution was selected with primary emphasis on desired characteristics of the boundary layer; the contour was derived as second step. It was known at that time that the boundary layer could be maintained laminar within a region of slight favourable pressure gradients; therefore, on aerofoils where the peak suction occurred far aft a decrease in frictional drag was to be expected. In fact, the N.A.C.A. low-drag aerofoils[1] attained a 30–50 per cent smaller minimum profile drag, depending on chordwise location of suction peak and Reynolds number, compared with wing sections of the older type. Since these aerofoils were widely known in the past and are today still used on a very large number of subsonic aircraft they provide a useful starting point for the

following reflections whose aim is to point out additional possibilities which have not yet been exploited*.

The emphasis in these considerations which are focussed on the old problem of obtaining minimum drag and maximum lift is placed less on deriving some specific designs than on discussing the basic principles to achieve boundary layer control by means of aerofoil geometry.

2. GENERAL CONSIDERATIONS

For a better understanding of what follows, some of the known relationships in connexion with the flow around aerofoil sections will be briefly recalled. Figure 1 shows the velocity distributions of three very different N.A.C.A. wing sections, which all possess the same maximum thickness chord ratios of 12 per cent. Aerofoil 0012 is a wing section of the older type; the other two sections, having peak suction further aft, are low-drag aerofoils of the N.A.C.A. 6 series.

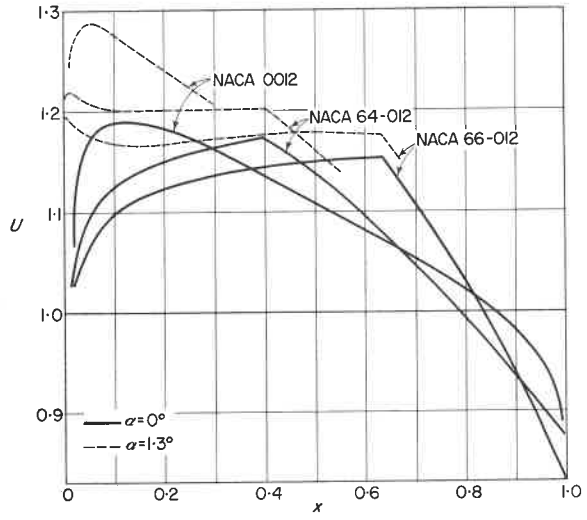

FIG. 1. Velocity distributions of three 12 per cent thick N.A.C.A. aerofoils at two angles of incidence.

The extensive favourable pressure gradient of low-drag aerofoils stabilizes the laminar boundary layer and delays transition until the region of highest supervelocity is reached. A corresponding decrease in frictional drag results. moving peak suction further aft is, however, no panacea since beyond the peak the unfavourable pressure gradient becomes steeper and steeper. The

* T. NONWEILER[2] has recently published a comprehensive review of the "state of the art" which includes supersonic and suction aerofoils not dealt with here.

load on the boundary layer which is turbulent within this region increases correspondingly. Finally, pressure drag increases at a higher rate than the frictional drag decreases, i.e. for a given aerofoil thickness and given Reynolds number there exists, in respect of drag, an optimum aft limit of the chordwise position of peak suction.

The effect of a positive setting of 1·3° on the velocity distribution over the suction side of the aerofoil section is shown in Fig. 1 by dotted line. For the low-drag aerofoils peak suction now occurs at the leading edge. The subsequent fall in velocity destabilizes the laminar boundary layer; the transition point can jump far forward and cause a sudden increase in drag. This process which occurs in the same way at negative angles of incidence is responsible for the characteristic indentation in the curve of profile drag of the section which is called "low-drag range" or "low-drag bucket"*. Older aerofoils, such as, for example, the already mentioned 0012 aerofoil, show, in general, no irregularities because the position of the transition point changes gradually and on the whole only very little.

The width of the low-drag bucket is closely connected with the minimum drag. If, as for example in Fig. 1, we start with a constant aerofoil thickness, it can be seen that section 66–012 has in fact the smallest drag because peak suction occurs further aft but, at the same time, it also has the narrowest low-drag bucket. With peak suction far aft the favourable pressure gradient becomes flatter and is more quickly transformed into an unfavourable one by increasing the angle of incidence than by an initially steeper favourable pressure gradient.

If, on the other hand, a certain aft position of the peak suction is maintained, the low drag range can, indeed, become wider with increasing aerofoil thickness, but the drag must also increase at the same time.

It can be seen that with N.A.C.A. low-drag aerofoils, almost irrespective of aerofoil type, a given width of the low-drag bucket is always associated with a given drag within the range. No advance can be claimed until this interdependence has been altered, i.e. until a smaller drag has been obtained with the same range or a wider low drag range has been achieved with the same drag.

In the following frequent reference will be made to comparable aerofoil sections. It is hereby assumed that either of the two named characteristics can form the basis of a comparison. The aerofoil thickness, important from a structural point of view, need not be considered separately since a certain aerofoil thickness is always necessary for a desired width of low-drag range whilst the reverse is not true.

With increasing Reynolds numbers the laminar boundary layer becomes less stable and the width of the low-drag bucket is reduced. The low-drag bucket can completely disappear at Reynolds numbers $Re > 10^7$. This

* In German "Delle".

numerical value relates to the Reynolds number formed by the aerofoil chord c and the free stream velocity U_∞.* When comparing experimental data it must be borne in mind that the width of the low-drag range is substantially dependent on the degree of turbulence of the free stream.

In general the minimum drag becomes smaller with increase of Reynolds number. This is the result of two opposing effects. An increase in Reynolds number reduces on the one hand the frictional drag referred to stagnation pressure and allows the boundary layer to become thinner and the already small pressure drag to become still smaller. On the other hand, the transition point can move forward due to the decreasing stability of the laminar boundary layer, thus causing an increase in minimum drag. Both effects are approximately equal for Reynolds numbers of the order $2-3\times10^7$; at larger Reynolds numbers one usually observes a slight increase in minimum drag.

The suitability of an aerofoil for high subsonic speeds is, in the first place, determined by its critical Mach number which itself mainly depends on the magnitude of the highest super-velocity. In general, a high critical Mach number is associated with a low super-velocity. Amongst those aerofoils of equal thickness given in Fig. 1 the N.A.C.A. 66 aerofoil, for example, will have the largest critical Mach number, not only at one angle of incidence but within a whole range of angles. The velocity distribution favourable to achieve a substantial region with laminar flow also helps to achieve a high critical Mach number†.

When exceeding the range of angles of incidence already mentioned velocity peaks occur at the wing leading edge which reduce the critical Mach number very rapidly. When plotting critical Mach number of a low-drag aerofoil against lift one obtains a characteristic indentation similar to the low drag bucket. For N.A.C.A. low-drag wing sections the same connexion is valid for this Mach number range as that expressed above for the low-drag range: almost independent of the type of aerofoil, a given critical Mach number is always associated with a given width and location of the Mach number range.

3. FURTHER DEVELOPMENT OF LOW-DRAG AEROFOILS

3.1. *M.R.-Aerofoils*

If magnitude and rear chordwise position of peak suction are the given design parameters, the velocity distribution upstream of the suction peak must be chosen so that it becomes constant on one side of the aerofoil at an angle of incidence α_1. The velocity gradient then remains positive for all

* The same definition applies to the rest of the text and the illustrations.

† The design of modern aircraft is frequently such that transition must set in at the leading edge of the wing. The choice of a low-drag aerofoil is in this case only justified by the higher critical Mach number of wing sections of this kind.

smaller angles of incidence and thus is favourable for maintaining the boundary layer laminar. When the velocity decrease aft of the suction peak is also prescribed, α_1 must be chosen compatible with the so-called condition of closure. In this case the low drag bucket becomes a maximum for these design parameters. The same should then also apply to the Mach number range.

Such M.R. (maximum range) wing sections, which otherwise are very similar to the N.A.C.A. sections, have been suggested by B. THWAITES[3] and amongst others, by M. J. LIGHTHILL[4]. In order to calculate the transition from one velocity distribution in potential flow $U(x)$ or $U(\phi)$ respectively at an angle of incidence α_1 to that at an angle of incidence α_2 one uses the well-known relation

$$\frac{U_1(\phi)}{U_2(\phi)} = \frac{\cos(\phi/2-\alpha_1)}{\cos(\phi/2-\alpha_2)}, \tag{1}$$

where the non-dimensional x-coordinate (with respect to the aerofoil chord) is the case of symmetrical aerofoils

$$x \approx \tfrac{1}{2}(1+\cos\phi), \qquad 0 \leqslant \phi \leqslant 2\pi \tag{2}$$

and α is measured from the zero lift angle.

When calculating the velocity distribution of M.R.-aerofoils one starts, of course, from the velocity assumed to be constant along a certain part of the chord at a certain given angle of incidence; velocity distributions for other angles are then calculated with the help of Eq. (1)*.

M.R.-sections give, theoretically, about 15–25 per cent greater low drag range than the N.A.C.A. low-drag aerofoils where the velocity does not, as shown in Fig. 1 by dotted lines, change monotonically into a constant distribution. Admittedly, the leading edge radius of M.R.-sections is even smaller than of the American wing sections, where a larger leading edge radius was retained in view of maximum lift. The question whether the M.R.-aerofoils exchange an increase of the low drag range for a reduction in maximum lift does not appear to have been examined experimentally. Theoretically one might even reach the opposite conclusion.

3.2. *Aerofoils of variable contour*

Within a given range N.A.C.A. low-drag aerofoils have a particularly small drag. W. PFENNINGER[5,5a] found a solution using different means. He chose

* In the more general case, treated especially by R. EPPLER[14] one wants to start not only from a single velocity distribution at one given angle of incidence but would wish to attain a number of velocity distributions along certain elements of the chord at several angles of incidence. For one particular element of the section one can, of course, stipulate certain distribution of velocity only for one angle of incidence; the velocity distributions for all other angles of incidence then follow for this element from Eq. (1).

for his design a very flat positive velocity gradient. Thus, the low-drag range is admittedly small but the maximum super-velocity and the velocity decrease towards the trailing edge also remain smaller than for the sections of the N.A.C.A. family, if the same aerofoil thickness and the same aft locations of peak suction are specified. Accordingly, conditions for the turbulent boundary layer are more favourable than in the case of the N.A.C.A. sections. The required width of the low-drag bucket is obtained by deflecting a small flap having a chord of about 10 per cent of the wing chord. As can be seen from Fig. 2 the combined effect of flap deflexion and change of angle of incidence is to alter, within certain limits, the velocity difference between upper and

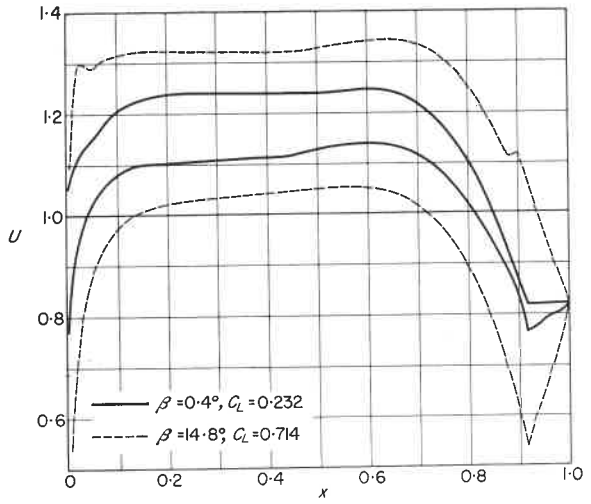

FIG. 2. Measured velocity distributions of a wing section designed by W. PFENNINGER. The aerofoil is 17 per cent thick and has a trailing edge flap of 0·10 chord. At $C_L = 0{\cdot}714$ the flap is deflected downwards by $\beta = 14{\cdot}8°$.

lower surface and hence the lift, but the difference remains almost constant along the chord. The favourable pressure gradient which is essential for keeping the boundary layer laminar, although small, can therefore, be maintained over a whole range of lift coefficients. Figure 3 shows that the drag of the 17 per cent thick Pfenninger wing section, having approximately the same width of the boundary bucket at $Re = 1{\cdot}5 \times 10^6$ as section N.A.C.A. 65–415, is about 13–14 per cent smaller. The lift-drag curve (polar diagram) of the Pfenninger section is the envelope of the individual lift-drag curves obtained with a constant flap setting β, the latter being varied within the range $-5{\cdot}4° \leqslant \beta \leqslant 16{\cdot}4°$.

A disadvantage of a flat positive pressure gradient is that it does not help much to stabilize the laminar boundary layer. Whilst on N.A.C.A. sections

a narrowing of the low-drag range is observed with increase of Reynolds number there is still a further reduction of minimum drag; with the Pfenninger type of aerofoil the low-drag bucket will disappear earlier and the minimum drag will rise prematurely. With regard to critical Mach number such shallow pressure distributions are, however, even more favourable than those of the N.A.C.A. 66 aerofoil of the same thickness.

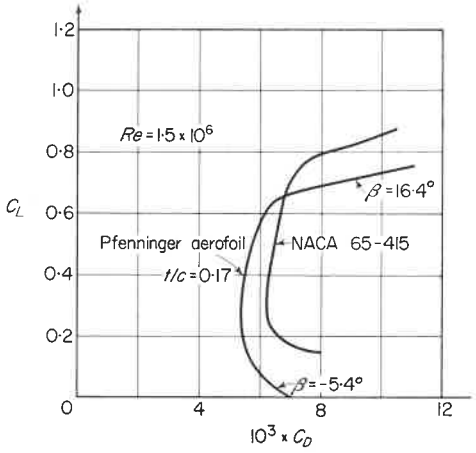

FIG. 3. Comparison of the lift-drag curves of a 17 per cent thick Pfenninger section with a 15 per cent thick N.A.C.A. section 65–415 at $Re = 1{\cdot}5 \times 10^6$. The lift-drag curve of the Pfenninger section is the envelope of individual lift-drag curves with fixed flap deflexions β, with β varied in the range:

$$-5{\cdot}4° \leqslant \beta \leqslant 16{\cdot}4°.$$

3.3. *Control of the turbulent boundary layer and the transition point*

The N.A.C.A. low-drag wing sections were developed with the primary object of keeping the boundary layer laminar over a certain chordwise distance. In this section it will be shown that careful control of the turbulent boundary layer and of the transition point by means of suitable velocity distributions can bring considerable additional improvements. As early as 1944 A. WALZ[6] studying the effect of contour changes calculated the influence on the velocity distribution and the boundary layer development of two modifications to the tail end of a symmetrical aerofoil section. He found that at $Re = 3 \times 10^7$ with a concave tail end (cusp) the turbulent boundary layer was thinner than when the tail end was convex. The shape parameter, indicative of separation, showed, however, an unfavourable trend in both cases; whilst with the convex tail end separation threatened at the trailing edge, with the concavely curved tail piece conditions were critical at the joint because there the decrease in velocity was unnecessarily large and steep.

The present author investigated independently in 1953 the influence of different velocity distributions on the development of the turbulent boundary layer within a region of rising pressure[7]. The main attention was devoted to those velocity distributions where the relevant turbulent boundary layer showed the least tendency to separate even at small Reynolds numbers. This is equivalent to stipulating that the shape parameter be constant throughout. Therefore, contrary to conventional usage, a boundary layer with specifically stipulated characteristics should be regarded as the starting point, rather than the velocity distribution.

Corresponding velocity distributions could, at first, only be obtained by trial and error using the approximative method developed by E. TRUCKENBRODT[8].

These velocity distributions, apart from reducing the danger of separation, resulted in a more favourable development of the turbulent boundary layer than the velocity distributions of the N.A.C.A. sections.

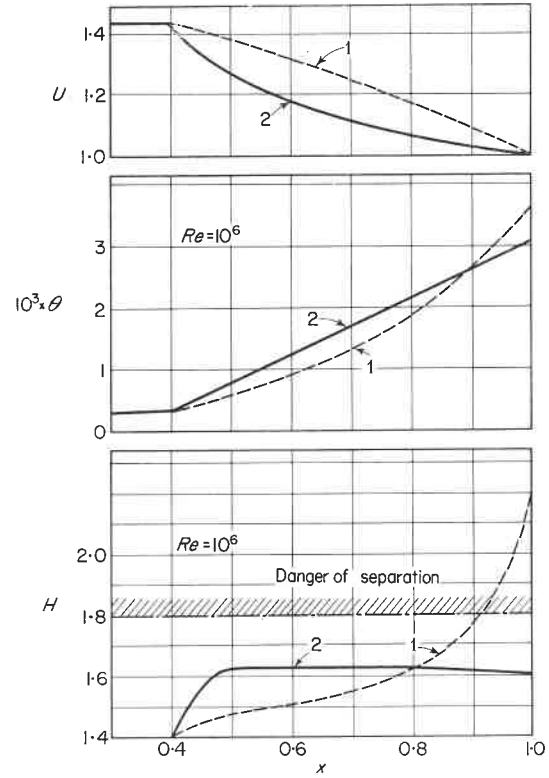

FIG. 4. Development of the turbulent boundary layer for two different velocity profiles. $Re = 10^6$; θ = momentum thickness; H = shape parameter.

Two results of these calculations are given in Fig. 4. Distribution 1, which corresponds to an N.A.C.A. aerofoil, results in a rapid increase of the shape parameter H and the momentum thickness θ at the trailing edge.

The situation is very different for distribution 2; here the gradient of momentum thickness and shape parameter remain practically constant, and the boundary layer thickness at the trailing edge is smaller than for the N.A.C.A. section.

Qualitatively, this result can also be directly derived from quadrature formulae which E. TRUCKENBRODT[8] has given for calculating the momentum thickness θ. If $U(x)$ is the non-dimensional velocity distribution and x_1 the position of transition point then, according to Ref. 8, introducing

$$C_1 = (U_1^3\theta_1)^{1\cdot17} \text{ and } D = 0\cdot00765\, Re^{-0\cdot167}$$

we have for the momentum thickness of the turbulent boundary layer in two-dimensional flow:

$$\theta = \frac{\left[C_1 + D\int_{x_1}^{x_2} U^{3\cdot33}\mathrm{d}x\right]^{0\cdot855}}{U_3} \equiv \frac{I}{U_3} \tag{3}$$

The integrand for the distribution 1 in Fig. 4 becomes, of course, greater than for distribution 2. Let the difference at the trailing edge be ΔI_{c1}. A negative velocity gradient similar to that of distribution 2 will be called in the remainder of the text "concave distribution" with shape parameter remaining constant at about $H \approx 1\cdot8$.

The importance of different boundary layer developments for the aerofoil drag can best be seen from the well-known formulae due to SQUIRE and YOUNG[9] and PRETSCH[10] which give the dimensionless drag value C_D. With suffix $_c$ indicating trailing edge:

$$C_D = 4\theta_c U_c^{\frac{1}{2}(5+H_c)} \approx 4\theta_c U_c^{3,4} \tag{4}$$

One must not overlook the fact that a velocity decrease typical for N.A.C.A. sections cannot be replaced simply by a concave distribution since otherwise an intersection of contours would occur upstream of the trailing edge. The velocity at the trailing edge must, therefore, be somewhat higher than for N.A.C.A. sections when a concave distribution is used. Moreover, this alteration does not affect the C_D value as much as might appear from Eq. (4); by inserting Eq. (3) in Eq. (4) one obtains

$$C_D \approx 4I_c U_c^{0\cdot4} \tag{5}$$

Increasing velocity at the trailing edge is equivalent to a slight flattening of the concave velocity gradient, whereby I_c is further reduced by an amount ΔI_{c2}. Experience has indicated that the increase in U_c and the reduction in I_c by ΔI_{c2} nearly compensate one another in Eq. 5, so that finally the difference ΔI_{c1} resulting in Fig. 4 affects the drag by almost the same amount.

The effective gain which can be obtained depends mainly on the aerofoil thickness. Approximately, it should be possible to obtain a percentage decrease of drag compared with N.A.C.A. sections which at Reynolds number of approximately 10^6 is as large as the percentage aerofoil thickness.

For the design of aerofoils it would be very useful if one could invert the calculation of the boundary layer and, starting from given shape parameters, calculate the shape of concave velocity distributions as a function of Reynolds number and chordwise position of the transition point. Furthermore, it should be possible to calculate in a reliable manner the development of $\theta(x)$ for different shape parameters and Reynolds numbers; for example when it is desired to determine an optimum velocity distribution. The author made an attempt in this direction[7] which, however, was inconclusive because the approximate methods used for calculating the turbulent boundary layer are too inaccurate in the special case of the concave velocity distribution. Before one can attempt tackling such problems, careful experimental research will have to be undertaken of the kind recently initiated by F. CLAUSER[16] and B. S. STRATFORD[17,18].

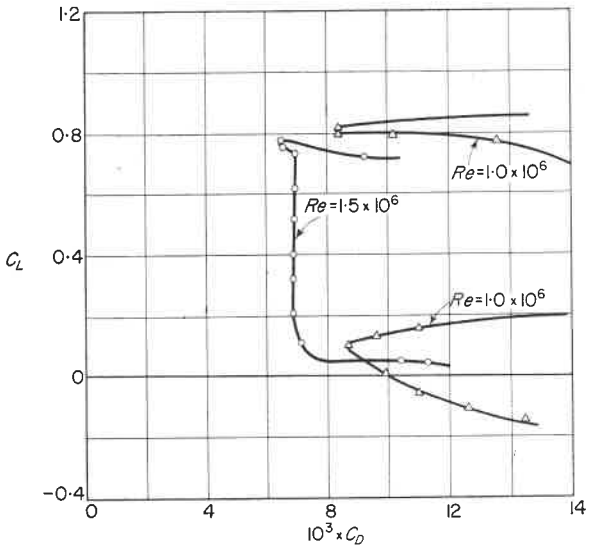

FIG. 5. Lift–drag curve of the 20 per cent thick aerofoil FX3 (Ref. 11) for two Reynolds numbers. At $Re = 1\cdot5 \times 10^6$ trip wires prevent the formation of a separation bubble. At $Re = 1\cdot0 \times 10^6$ the same wires are no longer effective and a separation bubble of about $0\cdot03c - 0\cdot05c$ width develops at $x = 0\cdot7c$.

Benefits will result not only from a rational treatment of the turbulent boundary layer but also from a suitable control of transition. On N.A.C.A. low-drag sections positive velocity gradient changes abruptly into a more or less steep negative velocity gradient. It is observed experimentally that at this point a separation bubble is formed, even at Reynolds numbers of the order 10^7, i.e. laminar separation occurs with subsequent reattachment on the upper surface of the aerofoil after the boundary layer has become turbulent. Formation of a separation bubble causes an unnecessary thickening of the initial turbulent boundary layer.

It is interesting to observe by experiment what happens when this separation bubble is removed by forced transition coinciding with the point of separation. F. X. WORTMANN[11] observed an increase in drag on the N.A.C.A. 64–418 section. B. H. CARMICHAEL[12] found that the drag did not change for the N.A.C.A. 66–621 aerofoil, i.e. with a steeper negative velocity gradient. With concave velocity distributions which have initially an extremely steep gradient a distinct reduction of drag was observed by moving the point of transition further upstream and avoiding the separation bubble.

In all these cases it would have been best, of course, if the position of the transition point had been left unchanged and if transition had occurred prior to separation. The need for such a control of transition becomes the more imperative the steeper the decrease of velocity is in the transition region. Such cases exist with concave distribution, and it is worth mentioning here that the velocity distribution on the upper surface of an aerofoil at large angles of attack, i.e. in the region of maximum lift, corresponds to a concave one (cf. Section 3.5).

What unpleasant effects a separation bubble which extends into a region of a steep negative velocity gradient may cause may be illustrated by Fig. 5. This shows the lift-drag curve of an aerofoil on which the positive velocity gradient changes directly into the steep negative gradient associated with the concave velocity distribution (cf. Ref. 11). At $Re = 1{\cdot}5 \times 10^6$ the separation bubble is removed by trip wires and the lift-drag curve shows normal character. At $Re = 1{\cdot}0 \times 10^6$ the trip wires are smaller than the critical roughness height and a separation bubble is formed which although of small size only, causes a very large increase in drag. It must be noted that the turbulent boundary layer aft of the bubble remained completely attached to the trailing edge.

F. X. WORTMANN[11] has found that it is possible to control transition by not connecting the positive and negative velocity gradients directly but by inserting between them a transition element called "instability range" where a flat negative velocity gradient occurs. By this means separation of the laminar boundary layer is avoided, but at the same time a high degree of instability of the (laminar) boundary layer is obtained.

For the instability range velocity distributions are chosen of the type

$$U = \alpha \bar{x}^m, \tag{6}$$

which, as is known, lead to so-called "similar" solutions of the boundary layer equations with constant shape parameter, α and m are suitable constants. For $m > -0{\cdot}091$ no separation of the laminar boundary layer occurs. The quantities α and $\bar{x}_1$ result from the conditions of continuity at point x_1 of the maximum velocity:

$$U(x_1) = U(\bar{x}_1) \text{ and } \theta(x_1) = \theta(\bar{x}_1).$$

Two parameters are decisive for determining the length of the instability range, the degree of turbulence of the free stream, i.e. the magnitude of the approaching perturbations and the rate at which such perturbations are amplified downstream of the instability point. In this connexion GRANVILLE[13] evaluated different measurements in a flow of very low turbulence. He found that in a positive pressure gradient

$$Re_{\theta t} - Re_{\theta i} \equiv \Delta Re_\theta \geqslant 400 \tag{7}$$

where Re_θ is the Reynolds number formed with momentum thickness; the suffixes t and i refer to the transition and instability points. For a rough estimate it is quite sufficient to calculate the difference ΔRe_θ from the chordwise position of highest super-velocity since the instability point falls near the maximum velocity as long as the velocity gradients, upstream and downstream of the peak suction, are not too small.

With this assumption the length of the instability range is given in Table I for several Reynolds numbers; it has further been assumed that the maximum velocity $U_1 = 1{\cdot}30$ occurs at $x_1 = 0{\cdot}5$ and that the velocity decrease causing instability follows from the equation

$$U = 1{\cdot}11\bar{x}^{-0{\cdot}09} \tag{8}$$

In addition, the resulting difference in velocity $U_1 - U_t$ at the beginning and end of the instability region is given.

TABLE I

Relationship between Re number, length of "instability range" and difference in velocities at the beginning and end of the instability range.

$Re = (U_\infty c)/\nu$	Δx	$U_1 - U_t$
1×10^6	0·400	0·132
4×10^6	0·200	0·087
9×10^6	0·133	0·069

Apart from the favourable initial conditions for the turbulent boundary layer the velocity decrease $U_1 - U_t$ which is possible without transition and

separation represents, especially at the smaller Reynolds numbers, a very desirable relief for the turbulent boundary layer. As has also been shown by the author[11] the function of the instability range is maintanied over a whole range of Reynolds numbers and even over the whole range of angles of incidence associated with the low-drag range. This insensitivity must be regarded as special advantage of the instability range.

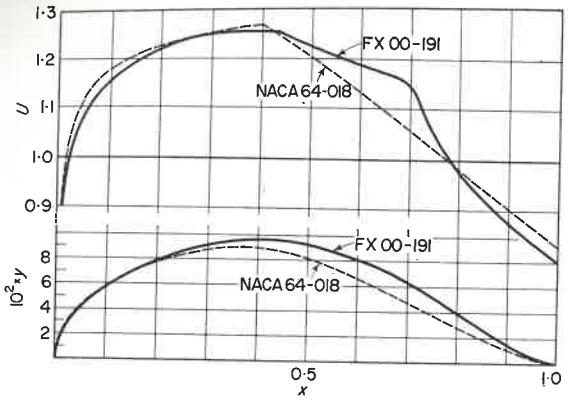

FIG. 6. Comparison of the velocity and thickness distributions of the N.A.C.A. 64–018 wing section with a 19·1 per cent thick FX aerofoil section. In the FX aerofoil the length of the instability range is determined for $Re = 2 \times 10^6$ and the concave velocity distribution of the steep negative gradient should, at the same Reynolds number, produce in the turbulent boundary layer a constant shape parameter $H = 1{\cdot}8$.

An example illustrating the application of ideas developed above is given in Fig. 6. The section was designed for a range of Reynolds numbers $1{\cdot}0 \times 10^6 \leqslant Re \leqslant 3 \times 10^6$. This section is compared with an N.A.C.A. wing section having approximately the same low-drag bucket. These two aerofoils were tested amongst others by the author[11] in a wind tunnel at $0{\cdot}7 \times 10^6 \leqslant Re \leqslant 1{\cdot}8 \times 10^6$. The results are presented in the form of polar diagrams for lift and drag in Fig. 7*. Figure 8 gives a summary of coefficients of minimum profile drag. It can be seen that the 19·1 per cent thick FX aerofoil has about 18 per cent less drag than the 18 per cent thick N.A.C.A. aerofoil. In addition, the maximum lift of the FX wing section seems to be somewhat greater than that of the N.A.C.A. aerofoil.

* For the sake of clarity only the velocity distributions of symmetrical wing sections are given in Fig. 6. The fact that the aerofoils in Fig. 7 had a small camber with constant lift distribution is unimportant for the comparison, since the character of the lift–drag curves, apart from a displacement to positive C_L values, remains practically unchanged.

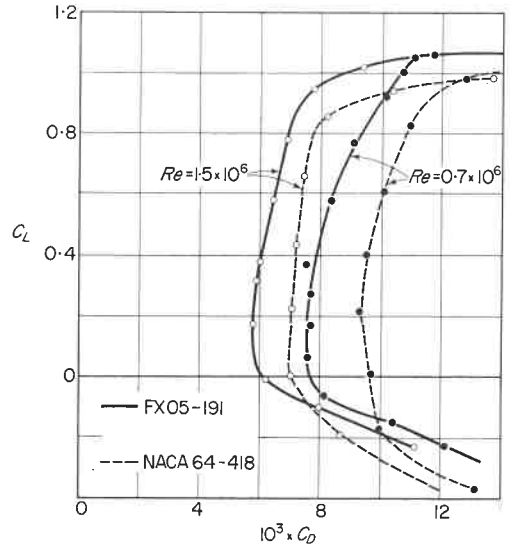

FIG. 7. Comparison of the lift-drag curves of the N.A.C.A. 64–418 and FX 05–191 wing sections at two Reynolds numbers (Ref. 11). The 19·1 per cent FX aerofoil has approx. 18 per cent smaller drag than the 18 per cent thick N.A.C.A. 64–418 aerofoil.

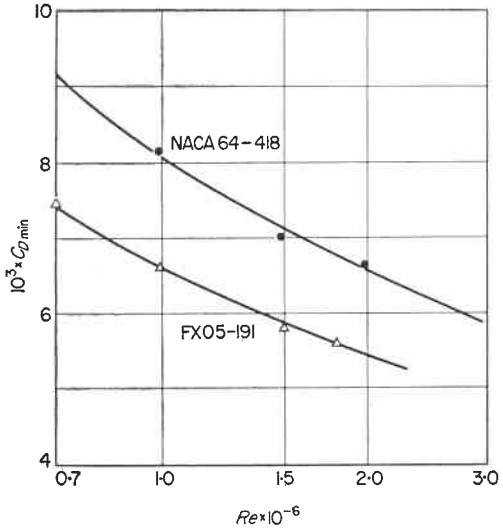

FIG. 8. Summary of the minimum profile drag coefficients in (Ref. 11) of sections N.A.C.A. 64–418 and FX 05–191 in relation to Reynolds numbers.

3.4. *Influence of lift distribution on minimum drag and the lift–drag curve of the wing section*

So far discussions were chiefly limited to symmetrical low–drag aerofoils or to such wing sections where in shock-free flow lift distribution remains practically constant along the aerofoil chord. Although a constant lift distribution moves the centre of the low–drag bucket to positive lift coefficients it has little influence on the width of the bucket and the minimum drag of a symmetrical section. Are thus all possibilities for reducing drag exhausted? Obviously not, since lift distribution can also have a considerable influence on drag. A cambered aerofoil can have less drag than a comparable symmetrical one.

This problem, numerically examined by the present author in his dissertation[7] is explained in more detail in Fig. 9. It should be noted that we are not dealing here with perfect and refined designs but only with five representative examples in which such refinements, as for example the insertion of instability ranges, were not incorporated. Apart from the lift coefficient, the selection is however not arbitrary; it follows logically within narrow tolerances when designing the sections with a positive velocity gradient for a stipulated extension of low drag range and a negative velocity gradient of predetermined, always similar shape parameter.

The lift or the difference in velocities ΔU on upper and lower surface is so varied that in Example (1) the whole lift is created on the rear half of the aerofoil and in Example (5) on the forward half of the aerofoil. Correspondingly, the moment of Section (1) is extremely large but that of Section (5) is very small. For Example (3) the lift distribution is constant.

The arithmetical mean of the rear chordwise positions of the suction peak on both sides of the aerofoil is practically the same for all examples. Hence the proportion of the whole surface over which the flow is laminar is approximately the same in all designs. In spite of this these aerofoils have drags of widely differing magnitude.

This is due partly to differing aerofoil thicknesses, partly to differing types of lift distributions. The latter influence can be seen when splitting the right hand side of Eq. (4), into the two different contributions to drag from upper and lower surface of the aerofoil:

$$C_D = (2\theta_c U_c^{3\cdot4})_{\text{upper}} + (2\theta_c U_c^{3\cdot4})_{\text{lower}} \qquad (9)$$

Therefore, on sections of type (1) in Fig. 9 a large momentum thickness is coupled with a low velocity on the lower surface over which the flow is turbulent; on the upper surface the thin boundary layer which has remained laminar is coupled with a large velocity at the trailing edge. The view of the favourable combination of boundary layer thickness and velocity at the trailing edge surprisingly small drag values are obtained by calculation for this aerofoil type (cf. Fig. 10 below).

The same combination occurs in aerofoil type (5). The drag values for this type must however be larger than those for type (1). This can readily be understood since it is known that the drag contribution of the concave distribution of type (1) is approximately twice that of the contribution from

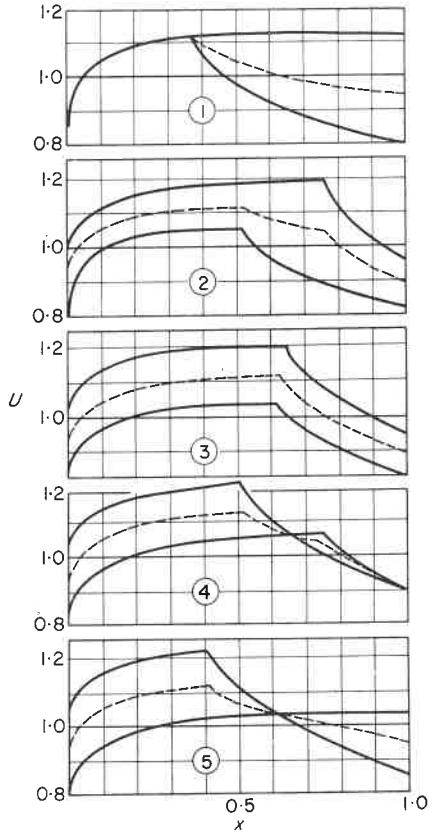

FIG. 9. Systematic variation of the lift distribution for five sample designs. The mean aft limit of the suction peak amounts to approximately 65 per cent of the chord. The concave distributions are calculated for an $H = 2{\cdot}1$ at $Re\ 2\times10^6$.

the upper surface in spite of the low velocity at the trailing edge. However, on aerofoil type (5), the whole level of the concave distribution is raised, since the lift is concentrated over the forward half of the aerofoil. The large drag contribution, therefore, becomes even larger and this increase cannot be compensated by a reduction of the already small drag contribution from the surface over which the flow is laminar.

However, by calculation, aerofoil type (5) should have a smaller drag than a symmetrical aerofoil with the same width of low-drag bucket*.

The situation is different for aerofoil type (3) with constant distribution of ΔU; its drag must be larger than that of a comparative symmetrical aerofoil. The increase in drag results simply from the fact that due to the constant lift distribution ΔU the boundary layer development remains practically unchanged; besides the following relation applies

$$U_c^{3\cdot4} < \tfrac{1}{2}(U_c+\tfrac{1}{2}\Delta U)^{3\cdot4}+\tfrac{1}{2}(U_c-\tfrac{1}{2}\Delta U)^{3\cdot4} \qquad (10)$$

where U_c is the velocity at the trailing edge of the symmetrical aerofoil. If the exponent had the value 3 instead of 3·4 the drag would increase proportionately to ΔU^2.

The calculated drag coefficients of the different aerofoils for $Re = 2\times10^6$ are given below in Fig. 10. As already mentioned at the beginning of this section, for all aerofoil types in Fig. 9 the negative velocity gradient is fixed

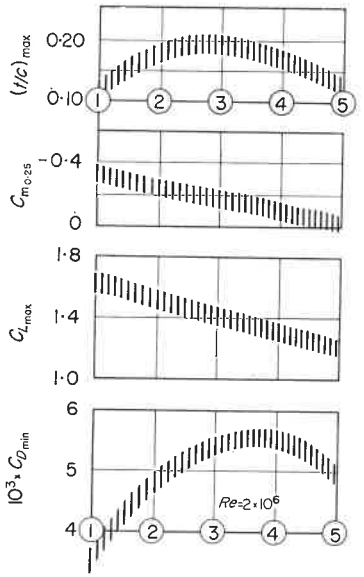

FIG. 10. Summary of calculated and estimated characteristics of the 5 designs of Fig. 9. The curves should not be taken as precise predictions but should indicate the trends resulting from the variation of the lift distribution on aerofoil characteristics.

* This is also confirmed experimentally; aerofoil N.A.C.A. 8–H–12 with fixed centre of pressure, whose velocity distribution corresponds to aerofoil type (5) has at $Re = 1\cdot8\times10^6$, a $C_D = 4\cdot8\times10^{-3}$. However, for the symmetrical aerofoil N.A.C.A., 64–012, which has the same thickness distribution and low drag range, $C_D = 5\cdot4\times10^{-3}$ at the same Reynolds number.

by a special stipulation, namely similar shape parameters for the turbulent boundary layer. Figure 10 shows the interesting result that by satisfying such a condition for the boundary layer the best aerofoils of great thickness are realized with lift distributions of the type (2) and (3) whilst other distributions lead to thinner aerofoils. This tendency simply results from the concave distribution; the total drop of velocity with two short concave distributions is greater than that of a single concave distribution extending over twice the length.

Up to now discussion has centred on the connexion between lift distribution and minimum drag; we should like now to deal briefly with the shape of the lift–drag curve outside the low-drag range. Aerofoil type (3) with constant lift distribution will behave in a very similar manner as a symmetrical low-drag aerofoil which is characterized by a sudden and large increase in drag when the low-drag range is exceeded. Only the symmetry of the drag increase is distorted on aerofoil type (3) due to the different velocities which occur on lower and upper surface. For lift coefficients greater than those associated with the low-drag bucket, drag will increase more rapidly, and more slowly for corresponding lower lift coefficients than in the case of a symmetrical section.

Aerofoils of types (1) and (5) are distinguished by having on each side of the section a velocity increase extending over almost the whole of the chord. If this rise is transformed by a fall of velocity due to a change in angle of incidence, causing transition to move upstream, the turbulent boundary layer of this side of the section (outside the low-drag range) meets with substantially more favourable conditions than, for example, on aerofoil type (3); the velocity distribution over the rear half of the section is without kink and has, on the whole, a shape similar to that of a concave distribution. Because of this profile drag increase to one or the other side of the low-drag bucket can be minimized.

This is specially important for aerofoil type (1) where the favourable velocity distribution is on the upper surface. With this type of aerofoil large angles of incidence, beyond the low-drag range, can be tolerated with attached turbulent boundary layer. If one also provides attached flow around the nose of the aerofoil (cf. next Section) this type, not only will profile drag be extremely low, but, in addition, a very high value of maximum lift will be reached. On the basis of such promising conceptions which were first expressed by the author[7], R. EPPLER[14] has recently submitted the design for such an aerofoil applying his method for aerofoil calculation. The large moment which is inevitably associated with such velocity distributions (cf. Fig. 10) stands in the way of general application of aerofoils of type (1).

A cambered wing section has, in general, a lower critical Mach number than a corresponding symmetrical section. It can be seen immediately from Fig. 9 that it is not constant lift distribution which is best in regard to critical

Mach number, as is sometimes maintained; the distribution of type (1) is most favourable and type (5) is least favourable in this respect.

Finally, it should be stressed that the foregoing reflections concerning the profile drag are not invalidated by the effect which the boundary layer may exert on the velocity distribution. It is true that the unsteady velocity jump at the trailing edge shown in Fig. 9 disappears due to the levelling effect of the boundary layer. However, whether transition to free stream velocity at the trailing edge takes place suddenly in form of a discontinuity or whether transition is more gradually spread over 5–10 per cent of the aerofoil chord, this does not effect the momentum thickness at a large distance downstrean of the aerofoil and therefore also not affects the drag.

3.5. *Control of the flow around the nose of the aerofoil*

At a large angle of incidence the laminar boundary layer may separate from the upper surface of the nose of the wing in form of a local separation bubble; the turbulent boundary layer may separate near the trailing edge thus forming an extensive wake. With further increase of angle incidence one can observe a very different behaviour in these two separation regions. The separation of the turbulent boundary layer may move slowly towards the leading edge thus limiting the maximum lift, or the laminar separation bubble can, after a critical angle has been exceeded, suddenly transform into a long bubble extending over the whole aerofoil chord and, in contrast to the first case, cause a sudden collapse of the lift. It is known today (cf., for example, P. R. OWEN and L. KLANFER[15]) that the laminar separation bubble remains short and hence innocuous as long as the Reynolds number Re_{δ}^{*} formed with the displacement thickness at the separation point remains greater than 400−500. In accordance with the observations in Section 3.4 (see Fig. 5), each bubble which occurs within a steep negative velocity gradient exerts an extremely unfavourable influence on the development of the turbulent boundary layer; care should, therefore, be taken *ab initio* in the design of an aerofoil to avoid laminar separation at the nose of the aerofoil. In other words, the velocity distribution over the upper surface of the aerofoil should be such that at high angles of incidence an instability range is formed near the leading edge. Therefore, exactly as in Section 3.4, the instability and separation points of the laminar boundary layer would have to be sufficiently drawn apart so that transition occurs near the separation point. An example is given in Figs. 11 and 12 to illustrate these points.

The full lines refer to the symmetrical section N.A.C.A. 63–015, the dotted lines to a modification of this aerofoil within $0{\cdot}002 \leqslant x \leqslant 0{\cdot}060$. The velocity distributions are shown in Fig. 11 for $\alpha = 0°$, and for the upper surface at $\alpha = 20°$. The dotted velocity distribution for $\alpha = 20°$ is also shown determined according to Eq. (6) for a constant shape parameter in the vicinity of the separation boundary.

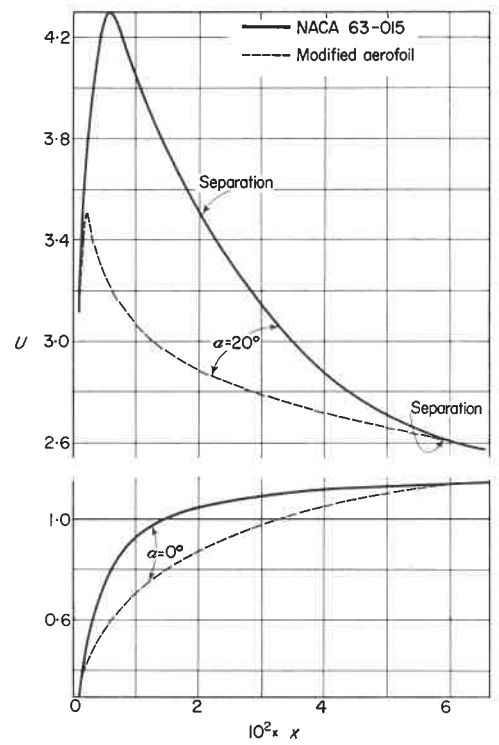

FIG. 11. Velocity distribution near the leading edge of section N.A.C.A. 63–015 and for a modified section. The lower curves are for $\alpha = 0°$, the upper ones for $\alpha = 20°$.

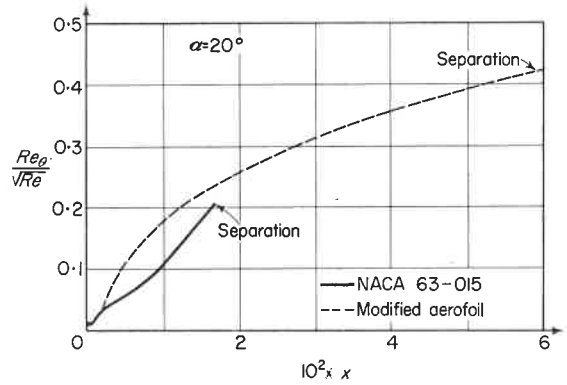

FIG. 12. Development of the displacement thickness with laminar flow near the leading edge of the N.A.C.A. 63–015 section and for a modified version. Angle of incidence $\alpha = 20°$. Calculation in each case is taken as far as the separation point.

The results of the boundary layer calculation are illustrated in Fig. 12. Separation of the laminar boundary layer for the N.A.C.A. aerofoil occurs already at $x = 0{\cdot}016$. Here $Re_{\delta^*}/\sqrt{Re} = 0{\cdot}8$, i.e. with $(Re_{\delta^*})_{\text{crit}} = 400$ the ensuing separation bubble would be innocuous for Reynolds numbers $Re \geqslant 0{\cdot}25 \times 10^6$ and followed by an attached turbulent boundary layer.

With the modified velocity distribution separation moves downstream to $x = 0{\cdot}06$. Now Re_{δ^*} is nearly doubled and the critical Reynolds number lowered to $Re \approx 0{\cdot}06 \times 10^6$. If one again assumes that the position of the instability point coincides with that of peak suction then the ratio $\Delta Re_\theta/\sqrt{Re}$ (up to the separation point) becomes 0·390, i.e. from $Re \approx 1 \times 10^6$ onwards the transition point can coincide with the separation point of the laminar boundary layer. At these Reynolds numbers, 6 per cent of the aerofoil chord suffice for rendering unstable the laminar boundary layer formed on the nose of the wing. The width of the low drag bucket is hardly affected by the slight modification to the velocity distribution.

The magnitude of the effective gain in maximum lift obtainable by carefully controlling laminar and turbulent boundary layers on the nose portion of the wing can be only assessed by wind tunnel tests*. In view of the rapid increase of flow velocities with increase of angle of incidence it is essential to calculate the shape of the nose very accurately and to construct the wing with corresponding precision.

It is immaterial whether the desired velocity distribution on the upper surface in Fig. 11 is obtained by choice of thickness distribution or shape of the camber line, or by a combination of both. It would thus be possible to obtain even with thinner aerofoils a velocity distribution similar to that in Fig. 11. However, with decreasing aerofoil thickness, it will be more difficult to avoid unfavourable velocity distributions at small angles of incidence on the lower side.

It may be argued that at high lift coefficients a turbulent boundary layer separating ahead of the trailing edge will affect the velocity distribution, based on potential theory, at the nose of the section. It is, however, not difficult to allow for this effect. It may perhaps suffice to bear in mind that separation at the trailing edge will cause all velocities on the upper surface of the wing nose to be lowered at about the same rate so that the shape of the instability range remains practically unchanged. It has already been mentioned that the instability range is relatively insensitive to small changes of flow conditions. One might therefore expect that this suggested method to increase maximum lift might prove practicable.

*At the Institut für Aerodynamik, T. H. Stuttgart, now begins experimental work in a new two-dimensional, low turbulence wind tunnel. A first low drag aerofoil especially designed with an instability range at the nose reached a maximum lift $C_L = 1{\cdot}65$ at $Re = 2 \times 10^6$. Similar aerofoils as the NACA 23012, 4412, 64–612, read at this Reynolds number $C_L = 1{\cdot}47$–$1{\cdot}50$.

CONCLUSION

Starting from the N.A.C.A. low-drag aerofoils the possibilities of further improvements have been discussed. THWAITES and LIGHTHILL have suggested wing sections which promise a wider low-drag bucket, and PFENNINGER has shown experimentally that aerofoils fitted with a flap can have less drag than comparable N.A.C.A. aerofoils. The author has recently developed the idea of selecting the velocity distribution entirely from theoretical considerations of boundary layer characteristics and not only in part, as in the case of the N.A.C.A. and M.R.-aerofoils, in order to obtain a further reduction in drag. The aim is not only for possible conditions favourable for the maintenance of a laminar boundary layer but also to control in a rational way transition as well as the development of the turbulent boundary layer. However, this advantage can only be fully exploited if transition can be forced to occur upstream of the steep negative gradient characteristic for a concave velocity distribution and if the formation of a separation bubble can be avoided. For controlling transition an instability range, which draws instability and separation points of the laminar boundary layer sufficiently apart, seems suitable. It provides a sufficiently large range of Reynolds numbers and angles of incidence within which it remains operational and especially at small Reynolds numbers it brings about a very desirable relief for the turbulent boundary layer. The first experiments made by the author showed that the practical application of these conceptions indicated a considerable reduction in the drag of low-drag aerofoils. This improvement was not obtained at the price of secondary disadvantages. It has been shown in detailed discussion that the lift distribution also has a strong influence on the drag and the shape of the lift-drag curve. In the last section a suggestion is made for using the instability range for increasing maximum lift.

REFERENCES

1. J. H. ABBOTT, A. E. v. DOENHOFF and L. S. STIVERS. Summary of aerofoil data, *N.A.C.A.*, Rep. 824 (1945).
2. T. NONWEILER. The design of wing sections, *Aircr. Engng.* (July 1956).
3. B. THWAITES. A new family of low drag wings with improved C_L–ranges, *A.R.C.*, R. & M. No. 2292.
4. M. J. LIGHTHILL. A new method of two-dimensional aerodynamic design, *A.R.C.*, R. & M. No. 2112.
5. W. PFENNINGER. Untersuchungen über Reibungsverminderungen an Tragflügeln, insbesondere mit Hilfe von Grenzschichtabsaugung, *Mitt. Inst. Aerodyn., Zürich*, No. 13.

5a. W. PFENNINGER. Experiments on a laminar suction aerofoil of 17 per cent thickness, *J. Aero. Sci.*, **16**, 227 (1949).

6. A. WALZ. Theoretische Widerstandsberechnung an einem Laminarprofil mit verschiedenen Schwanzteilformen, *U.M.*, 3131 (1944); vgl. auch F. W. RIEGELS, *Aerodynamische Profile*, p. 107, München (1958).

7. F. X. WORTMANN. Ein Beitrag zum Entwurf von Laminarprofilen für Segelflugzeuge und Hubschrauber, *Z.f.W.*, **3**, 333 (1955). British M.O.S. translation TIL/T A903.
8. E. TRUCKENBRODT. Ein Quadraturverfahren zur Berechnung der turbulenten und laminaren Reibungsschicht, *Ing.-Arch.*, **20**, 211 (1952).
9. H. B. SQUIRE and A. D. YOUNG. The calculation of the profile drag of aerofoils, *A.R.C.*, R. & M. No. 1838.
10. J. PRETSCH. Zur theoretischen Berechnung des Profilwiderstandes, *Jbh. Dtsch. Luftfahrtforsch. I.*, p. 61 (1938).
11. F. X. WORTMANN. Experimentelle Untersuchungen an neuen Laminarprofilen für Segelflugzeuge und Hubschrauber, *Z.f.W.*, **5**, 228 (1957). British M.O.S. translation TIL/T A906.
12. B. H. CARMICHAEL. Experimental investigation of a thick laminar aerofoil, *Soaring*, **22**, 6 (Nov. 1958).
13. P. S. GRANVILLE. The calculation of viscous drag of bodies of revolution, *David Taylor Model Basin*, Rep. No. 849 (1953); vgl. auch H. SCHLICHTING, *Grenzschichttheorie*, p. 391, Karlsruhe (1958).
14. R. EPPLER. Direkte Berechnung von Tragflügelprofilen aus der Druckverteilung, *Ing.-Arch.*, **25**, 56 (1957).
15. P. R. OWEN and L. KLANFER. On the laminar boundary layer separation from the leading edge of a thin aerofoil, *A.R.C.*, Current Paper No. 220.
16. F. H. CLAUSER. Turbulent boundary layers in adverse pressure gradients, *J. Aero. Sci.*, **21**, 91 (1954).
17. B. S. STRATFORD. The prediction of separation of the turbulent boundary layer, *J. Fluid. Mech.*, **5**, 1 (1959).
18. B. S. STRATFORD. An experimental flow with zero skin friction throughout its region of pressure rise, *J. Fluid Mech.*, **5**, 17 (1959).